Fiber-based optical parametric amplifier for 40-Gb/s NRZ-DPSK signal transmission system employing QC-LDPC codes

Jian Zheng (郑 健)[1,3*], Hongxia Bie (别红霞)[1], Xuekun Zhang (张雪坤)[1], Chunyang Lei (类春阳)[1], Ming Fang (房 明)[1], Sha Li (李 莎)[2], and Zhe Kang (康 哲)[2]

[1]*School of Information and Communication Engineering, Beijing University of Posts and Telecommunication, Beijing 100876, China*

[2]*State Key Laboratory of Information Photonics and Optical Communications, Beijing University of Posts and Telecommunication, Beijing 100876, China*

[3]*Department of Medical Information Engineering, Zunyi Medical College, Zunyi 563003, China*

[*]*Corresponding author: dotopala@hotmail.com*

Received June 6, 2013; accepted September 16, 2013; posted online November 6, 2013

In this letter, we investigate quasi-cyclic low-density parity-check (QC-LDPC) codes in a 40-Gb/s nonreturn-to-zero differential phase-shift keying (NRZ-DPSK) signal transmission system based on a fiber-based optical parametric amplifier (FOPA). A constructed algorithm of QC-LDPC codes according to the optimizing set of shift values on the circulant permutation matrix (CPM) of the basis matrix is proposed. Simulation results prove that the coding gain in the encoded system can be realized at 10.2 dB under QC-LDPC codes with a code rate of 5/6 when the bit error rate (BER) is 10^{-9}. In addition, the error-floor level originating from the uncoded system is suppressed.

OCIS codes: 060.0060, 220.0220, 230.0230.
doi: 10.3788/COL201311.110601.

An optical communication network has several advantages such as a large capacity, long-haul optical transmission systems, and powerful anti-interference ability. However, several factors, such as signal attenuation, fiber nonlinearities, dispersion, and system defects, can distort optical signals, result in error bits, and degrade the performance of a fiber optical transmission system.

To overcome the effects of these factors, forward error correction (FEC)[1−3], such as Reed–Solomon (RS) codes[1], RS-concatenated codes[2], and turbo codes[2], has been introduced to optical transmission systems. Meanwhile, coding gain achieves a high level, i.e., more than 10 dB[2]. Low-density parity-check (LDPC) codes are widely used in optical communication systems because of their superior performance[4−7]. Vasic *et al.*[4,5] show that LDPC codes improve the bit error rate (BER) performance of optical transmission systems; however, the encoding algorithm of LDPC codes is fairly complex. Quasi-cyclic LDPC (QC-LDPC) codes have been widely applied to optical transmission systems in recent years because of their simpler encoding structure compared with LDPC codes[8−11]. Milenkovic *et al.*[11] presented a class of QC-LDPC with six girths (a girth represents the shortest cycle in a Tanner graph) and applied it to an optical transmission system based on an erbium-doped fiber amplifier (EDFA); a coding gain of 11 dB was achieved when the BER was 10^{-9}. However, EDFA can only amplify signals within the 1550-nm wavelength band and accompanies uneven gain bandwidth and optical surge.

Fiber-based optical parametric amplifier (FOPA) is a well-known technique that not only can provide distributed or lumped gain through high-nonlinearity optical fibers, but also offers wide gain bandwidth, arbitrary wavelength amplification, and 0-dB noise figure amplification[12]. However, the performance of FOPA can be impaired by pump jitters and phase mismatches. Therefore, the problem of overcoming such effects in FOPA-based optical transmission systems has become the focal point of research.

In this study, we aim to correct error codes caused by system defects, fiber nonlinearity, and dispersion effects by using FEC. We present a constructed algorithm of QC-LDPC codes that ensures maximization of girth in the corresponding Tanner graph by optimizing the set of shift values on the circulant permutation matrix (CPM) of the basis matrix. The QC-LDPC codes are applied to a 40-Gb/s nonreturn-to-zero differential phase-shift keying (NRZ-DPSK) signal transmission system based on FOPA. The simulation results prove that: 1) the coding gain in the encoded system can achieve 10.2 dB under QC-LDPC codes with a code rate of 5/6 when the BER is 10^{-9}, 2) the error-floor level originating from the uncoded system is suppressed effectively.

In particular, QC-LDPC codes can be important as algebraically constructed LDPC codes. Compared with LDPC codes, QC-LDPC codes have the following advantages: 1) a special encoding structure, which can be implemented by a shift register; 2) a highly efficient parallel decoding algorithm, which is based on protographs known as Tanner graphs. These features are highly suitable for optical transmission systems. Although QC-LDPC codes can exhibit perfect performance, they are susceptible to short cycles in Tanner graphs. Hence, we propose an algorithm to maximize the girth of QC-LDPC codes.

The general idea of the algorithm presented in this letter vis as follows. We started with a basis matrix constructed by the improved progressive edge-growth[13] al-

gorithm. We then selected a shift value of the CPM of the basis matrix that can be divided simply into the following four steps. 1) The cycle set of each CPM of the basis matrix was searched one by one. 2) The candidate set of the shift value of each CPM was computed. 3) The candidate set was optimized. 4) A number was selected from the candidate set as the shift value for each CPM of the basis matrix. This procedure would ensure that the cycle is larger than the desired girth. However, when we computed the candidate set, several shift values were obtained for the same CPM. Therefore, selecting a suitable number for the CPM from the set became the key point of the proposed algorithm, i.e., optimizing the candidate set. The optimizing procedure is described as follows.

A QC-LDPC code could be defined as a $c \times t$ basis matrix with elements that represent a zero matrix or a CPM p^{x_i}. p^{x_i} was obtained from a $p \times p$ identity matrix by cyclically shifting the identity matrix to the right by x_i times for any integer x_i, $0 \leqslant x_i < p$. The parity-check matrix H of QC-LDPC codes was a $cp \times tp$ matrix. The corresponding Tanner graph of the basis matrix was defined as $G = (V \cup C, E)$, where $V = \{v_1, \cdots, v_t\}$ and $C = \{c_1, \cdots, c_c\}$ represent the variable nodes and the check nodes, respectively; E represents the edge set of the Tanner graph that includes all edges in the graph; e represents one of the edge set in E, where $e = (v_i, c_j | v_i \in V, c_j \in C) \in E$. Each column and row in the basis matrix corresponded to the variable nodes and check nodes of the Tanner graph, respectively.

Given a basis matrix, the corresponding parity-check matrix was calculated based on the following argument. For each potential cycle on each CPM of the basis matrix, we passed each shift value of the CPM in the potential cycle and marked the values that would not result in a potential cycle. All other shift values in the potential cycle were assumed to remain unchanged. For example, for six potential cycles, six cycles would exist if $p^{[\sum_{i=1}^{6}(-1)^{i-1}x_i] \bmod p} = 1$, i.e., $[\sum_{i=1}^{6}(-1)^{i-1}x_i] \bmod p = 0$, where $x_1 - x_6$ represent the shift values. Assuming that $x_1 - x_5$ remained unchanged, we computed the candidate set of x_6 and determined the values that could form six cycles in the check matrix. If $\{[\sum_{i=1}^{5}(-1)^{i-1}x_i] - x_6\} \bmod p \neq 0$, where $0 \leqslant x_6 < p$, then we could obtain the candidate set that ensures a cycle length larger than the six cycles in the check matrix.

Based on the preceding description, when the cycle length formed in the check matrix was larger than six, several CPMs of the basis matrix would overlap in the same cycle. This condition would make the algorithm complicated. However, when the girth was eight in the optical communication system, the QC-LDPC codes exhibited a perfect performance. Hence, we focused on eliminating four and six cycles in this study.

The aim of the algorithm is to optimize the candidate set of the CPM. The algorithm for optimizing the aforementioned candidate set is described as follows.

• Step 1: The variable node V_i is initialized according to the degree distribution d_i.

• Step 2: The k_{th} shift value of the CPM on the variable node V_i is searched and defined as V_i^k.

• Step 3: If $k = 1$, then $V_i^1 = \text{random}(x)$ and $0 \leqslant x < p$, where random is a function that randomly selects an integer from x.

• Step 4: If $2 \leqslant k \leqslant d_i$,

—then all cycles related to V_i^k are searched and a set $V_i^k(l)$ is defined, where l represents the cycle length formed in the check matrix;

—then the candidate set of the shift value on V_i^k is calculated, i.e., $N_{V_i^k}(l) = \left\{ ||x \sum_{i=1}^{l-1}(-1)^{i-1}x_i - x| \bmod p \neq 0 \right\}$;

—then the intersection of $N_{V_i^k}(l)$ is calculated, i.e., $\Gamma = \bigcap_{l=4}^{l_{\max}} N_{V_i^k}(l)$, where $l_{\max}$ is the longest cycle in $V_i^k(l)$.

—if $\Gamma = \varphi$, then $l_{\max} = l_{\max} - 2$ and the preceding step is repeated.

—if $|\Gamma| \geqslant 1$, then $V_i^k = \text{random}(\Gamma)$, where $|\Gamma|$ indicates the number of Γ.

• Step 5: The CPM on V_i is checked to determine if it has been processed; if not, then $k = k + 1$ and step 4 is repeated.

The girth of the QC-LDPC codes constructed by the aforementioned algorithm can arrive at 6. As the code length increases, the girth can arrive at 8.

To validate the performance of QC-LDPC codes in optical communication systems, we constructed a 40-Gb/s NRZ-DPSK signal transmission system based on FOPA by using the software Virtual Photonics Integrated (VPI), as shown in Fig. 1. The input 40 Gb/s electrical signal was first modulated onto an optical carrier with an average power and central wavelength of 0.01 mW and 1316 nm, respectively, and a NRZ-DPSK format for electrical/optical conversion. The modulated optical signal was launched into a single-mode fiber (SMF) for the performance degeneration with 110 km. The power of the output optical signal was fairly low because of the attenuation and dispersion effects in the SMF. Thus, FOPA that consisted of a 50-m high-nonlinearity fiber (HNLF) with zero dispersion at 1305.5 nm and a pump at 1305 nm was selected to amplify the signal. A high gain with a 0-dB noise figure can be obtained easily with the action of the parametric amplifier. Before amplification was performed in FOPA, a part of the output optical signal from the SMF was delivered into a phase-locked loop with a 99/1 coupler and a photoelectric detector to control the pump phase in FOPA. The optical signal was filtered by an optical band-pass filter at the output port of the HNLF for NRZ-DPSK optical demodulation.

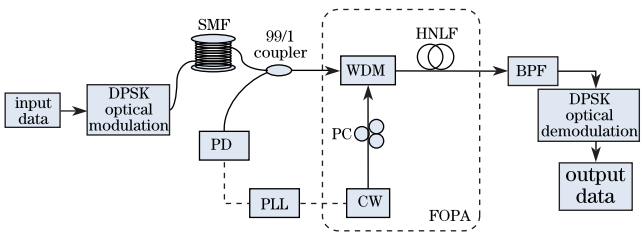

Fig. 1. 40-Gb/s NRZ-DPSK signal transmission system based on FOPA. PD: photoelectric detection; PLL: phase lock loop; WDM: wavelength-division multiplexing; PC: polarization controller; CW: continuous wavelength laser; BPF: band pass filter.

Uncoded pseudo-random codes (504 bits) were transmitted through the system. These data were carried on a relative phase of the optical carrier with a center wavelength of 1316 nm. The phase of the optical carrier would be distorted by dispersion, nonlinearity, and other problems during transmission in the fiber. The imperfect fiber would produce error bits. The amplification of FOPA was based on a highly efficient four-photon mixing that relies on the relative phase among the four interacting photons. The pump light and the optical signals were coupled by wavelength-division multiplexing and forwarded into the 50-m HNLF. We established the pump wavelength near the zero-dispersion wavelength of the HNLF to realize phase matching. The band-pass filter with a center wavelength of 1316 nm was used to divide the amplified signal. However, the amplification process could not satisfy phase matching at any time; phase factor θ could not always be $\pi/2$. Thus, error bits, which were caused by pump jitter and phase mismatching, occurred. The electrical signal after the DPSK optical demodulation module suffered from severe fluctuations caused by pump jitter, dispersion, nonlinearity, and other factors. Hard-decision decoding led to high BERs and inefficient communication performance. The received optical power versus the BER is shown in Fig. 2.

As shown in the figure, the BER would arrive at 10^{-6} with an error floor when the received optical power was –15 dB. To improve performance and to suppress the error-floor level, we added a QC-LDPC code encoder and decoder in the system, as shown in Fig. 3.

We then verified the performance of the QC-LDPC codes. We first constructed a FOPA-based 40-Gb/s NRZ-DPSK signal transmission system through VPI. We wrote the encoder and the decoder by C language and constructed a group of QC-LDPC codes according to the algorithm presented in this letter. We obtained the numerical results by using Monte Carlo simulations with the QC-LDPC code decoder to a maximum of 30 iterations for the belief propagation (BP) algorithms. When the number of iterations exceeded 30 or the frame errors arrived at 100, the BP algorithm was terminated.

Example 1: We considered the BER performance of QC-LDPC codes with different code rates in the FOPA-based 40-Gb/s NRZ-DPSK signal transmission system. The SMF-28, pump wavelength, and amplifier gain were 90 km, 1305 nm, and 20 dB, respectively. The code length of the QC-LDPC codes was $n = 4080$, with code rates of 1/2, 2/3, and 5/6, and basis matrices of 12×24, 8×24, and 4×24, respectively. The size of the CPM was $p = 170$. The girths of QC-LDPC codes with different code rates were 8, 6, and 6. The BER curves of the uncoded or encoded codes versus the received optical power are depicted in Fig. 4. As shown in Fig. 4, the coding gain with a code rate of 5/6 arrived at 10.2 dB when the BER was 10^{-9}.

Example 2: We tested the BER performance of SMF-28 with different lengths in the system with the same parameters as those in Example 1. The QC-LDPC codes had a code length of 4080, a code rate of 5/6, a basis matrix of 4×24, a CPM size of 170, and a girth of 6. The starting length of SMF-28 was 110 km. The fiber length increased gradually, with a step size of 20 km. The BER performances of SMF-28 with different lengths are depicted in Fig. 5. The BER performances degraded with increasing SMF-28 length because of fiber nonlinearities and dispersion effects. When the SMF-28 length was

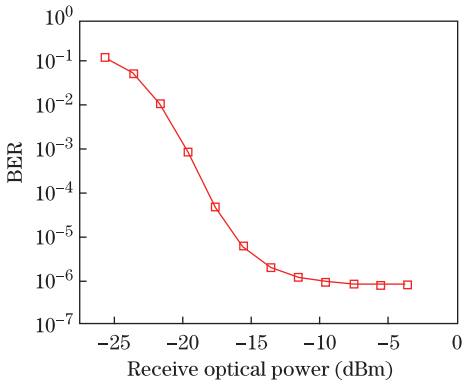

Fig. 2. Received optical power versus the BER by hard-decision decoding.

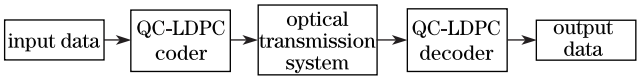

Fig. 3. FOPA-based 40-Gb/s NRZ-DPSK signal transmission system with an encoder and a decoder for QC-LDPC codes.

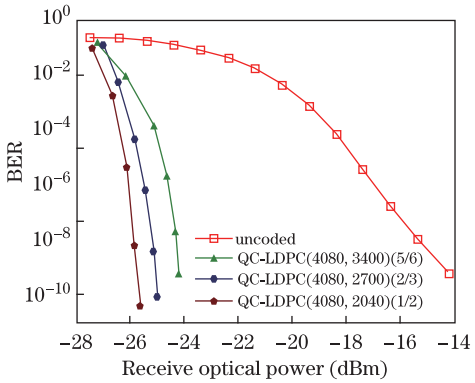

Fig. 4. (Color online) BER performances of QC-LDPC codes with different code rates in the FOPA-based 40-Gb/s NRZ-DPSK signal transmission system.

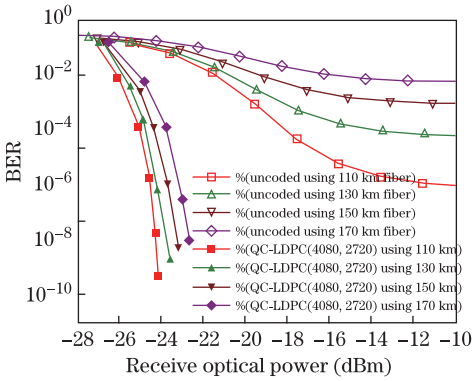

Fig. 5. (Color online) BER performances of QC-LDPC codes with different SMF lengths in the FOPA-based 40-Gb/s NRZ-DPSK signal transmission system.

170 km, the BER was approximately 10^{-2}. The BER performances were obviously improved by QC-LDPC codes, and the error floor originating from the uncoded hard decision was suppressed.

In conclusion, we investigate the performance of QC-LDPC codes in a 40-Gb/s NRZ-DPSK signal transmission system based on a FOPA. The impairments originating from pump jitter, phase mismatch, fiber nonlinearity, and dispersion are overcome. We also present a constructed algorithm of QC-LDPC codes according to the optimizing shift values of the CPM of the basis matrix, by which the girth of the Tanner graph can arrive at 6 or 8. The BER performances of QC-LDPC codes with different code rates and fiber lengths are tested in this system. The simulation results indicate that QC-LDPC codes can correct error codes caused by fiber nonlinearities, dispersions, pump jitters, and phase mismatches.

This work was supported by the National Natural Science Foundation of China (No. 41174158) and the National Commonwealth Research Project of China (No. 201011081-4).

References

1. J. L. Pamart, E. Lefranc, S. Morin, G. Balland, Y. C. Chen, T. M. Kissell, and J. L. Miller, Electron. Lett. **30,** 342 (1994).
2. T. Mizuochi, Y. Miyata, T. Kobayashi, K. Ouchi, K. Kuno, K. Kubo, K. Shimizu, H. Tagami, H. Yoshida, H. Fujita, M. Akita, and K. Moto-shima, IEEE J. Sel. Top. Quantum Electron. **10,** 376 (2004).
3. D. Han, L. Xi, M. Li, H. Chen, and F. Liu, Chin. Opt. Lett. **9,** 070604 (2011).
4. B. Vasic and I. B. Djordjevic, IEEE Photon. Technol. Lett. **14,** 1208 (2002).
5. B. Vasic, I. B. Djordjevic, and R. Kostuk, J. Lightwave Technol. **21,** 438 (2003).
6. Y. Wu, A. Yang, L. Feng, and Y. Sun, Chin. Opt. Lett. **11,** 030601 (2013).
7. Y. Wu, A. Yang, Y. Sun, and Q. Zhao, Chin. Opt. Lett. **10,** s10605 (2012).
8. M. Arabaci, I. B. Djordjevic, R. Saunders, and R. M. Marcoccia, IEEE Photon. Technol. Lett. **22,** 434 (2010).
9. D. Chang, F. Yu, Z. Xiao, Y. Li, N. Stojanovic, C. Xie, X. Shi, X. Xu, and Q. Xiong, in *Proceedings of Optical Fiber Communication Conference and Exposition* (*OFC/NFOEC*) OTuN2 (2011).
10. Y. Zhang, M. Arabaci, and I. B. Djordjevic, Opt. Express **20,** 9296 (2012).
11. O. Milenkovic, I. B. Djordjevic, and B. Vasic, IEEE J. Sel. Top. Quantum Electron. **10,** 294 (2004).
12. J. Hansryd, P. A. Andrekson, M. Westlund, J. Li, and P. Hedekvist, IEEE J. Sel. Top. Quantum Electron. **8,** 506 (2002).
13. H. Xiao and A. H. Banihashemi, IEEE Commun. Lett. **8,** 715 (2004).